Proc. Natl. Acad. Sci. USA
Vol. 94, pp. 1224–1229, February 1997
Developmental Biology

Microtubule-mediated transport of organelles and localization of β-catenin to the future dorsal side of *Xenopus* eggs

BRIAN A. ROWNING*†‡, JONATHAN WELLS‡, MIKE WU‡, JOHN C. GERHART‡, RANDALL T. MOON*, AND CAROLYN A. LARABELL†§

*Howard Hughes Medical Institute and Department of Pharmacology, University of Washington School of Medicine, Seattle, WA 98195; and †Lawrence Berkeley National Laboratory and ‡Department of Molecular and Cell Biology, University of California, Berkeley, CA 94720

Communicated by John C. Gerhart, December 3, 1996

ABSTRACT **The dorsal–ventral axis in frog embryos is specified during the first cell cycle, when the cortex rotates relative to the cytoplasmic core along parallel microtubules associated with the core. Cytoplasmic transfer experiments suggest that dorsal determinants are transported 90° from the vegetal pole to the dorsal equator, even though the cortex rotates only 30°. Here we show that, during rotation, small endogenous organelles are rapidly propelled along the subcortical microtubules toward the future dorsal side and that fluorescent carboxylated beads injected into the vegetal pole are transported at least 60° toward the equator. We also show that deuterium oxide, which broadens the zone of dorsalization even though it reduces the extent of rotation and is known to randomize the microtubules, also randomizes the direction of organelle transport. Moreover, β-catenin, a component of the Wnt signaling pathway that possesses dorsalizing activity in *Xenopus*, colocalizes with subcortical microtubules at the dorsal side of the egg at the end of rotation. We propose that cortical rotation functions to align subcortical microtubules, which then mediate the transport of dorsal determinants toward their plus ends on one side of the egg.**

In frog eggs, the cortex rotates ≈30° relative to the cytoplasmic core during the first cell cycle, and the side toward which the vegetal pole cortex rotates (usually opposite the sperm entry point) always becomes the dorsal side of the embryo. Rotation is accompanied by a parallel array of microtubules just inside the cortex (1), and, if cortical rotation is blocked by microtubule inhibitors, the embryo develops only ventral organization, with no dorsal or anterior features. On the other hand, if a normal egg is manually tipped or centrifuged midway through the first cell cycle to force a second rotation, a second axis can be produced, leading in the most dramatic cases to a two-headed tadpole (2, 3).

A second axis also can be produced by taking cytoplasm from the vegetal pole before rotation (or from the equator on the prospective dorsal side after rotation) and injecting it into the ventral equatorial region of an egg that otherwise would form only one axis (4, 5). Furthermore, removal of the vegetal pole region before, but not after, rotation generates ventralized embryos (6). These experiments suggest that dorsalizing components are transported ≈90° from the vegetal pole to the equator even though the cortex rotates only ≈30° during cortical rotation. Any hypothesis of how cortical rotation produces dorsalization should account for this difference.

An adequate hypothesis also should explain the anomalous results obtained by treating frog eggs with deuterium oxide (^2H_2O). Treatment with 70% ^2H_2O soon after fertilization often broadens the zone of dorsalization; the resulting embryos are characterized by enlarged heads and, in the most extreme cases, by circumferential eyes and cement glands. ^2H_2O also tends to reduce the extent of cortical rotation by inducing the precocious formation of a random subcortical meshwork of microtubules rather than a parallel array (7). Yet, reducing the extent of cortical rotation with microtubule inhibitors such as UV light produces ventralized embryos, which lack dorsal and anterior structures in proportion to the reduction in rotation (2, 3). Why does reducing the extent of cortical rotation with ^2H_2O result in broadening of the zone of dorsalization whereas reducing its extent with UV light results in ventralization? Using confocal microscopy of living eggs, we found that small organelles and carboxylated beads are transported along the microtubules for distances greater than 30° toward the future dorsal side of the egg during cortical rotation. In addition, this transport becomes randomized in the presence of ^2H_2O. We propose that it is the microtubule-directed delivery of dorsalizing components to one equatorial sector of the normal egg that is responsible for dorsal–ventral axis specification.

Although the identity of the dorsal determinant(s) is unknown, likely candidates include components of the Wnt signaling pathway because they are present maternally (8) and are known to promote duplication of the embryonic axis if injected in the equatorial region of the egg (9–13). We focused on β-catenin, a downstream protein of this pathway, because it has been shown to be both necessary (14) and sufficient (13, 15) for formation of dorsoanterior structures. In addition, it has recently been shown that there are dorsal–ventral differences in the expression of β-catenin after the midblastula transition (16). In this paper, we show that, by the end of cortical rotation, β-catenin is localized on the dorsal side in the layer containing the microtubules of the parallel array. The dorsal, vegetal β-catenin observed here may arise through any of several mechanisms, including a stabilization of β-catenin on the prospective dorsal side, increasing its availability for interaction with the microtubules and perhaps contributing to the increased levels of β-catenin seen in dorsal blastomeres during subsequent cleavage stages (17).

MATERIALS AND METHODS

Preparation of Eggs and Embryos. Adult frogs (*Xenopus laevis*) were raised in the laboratory and fed trout chow (Purina) twice a week. Ovulation was induced by injecting 800 units of human chorionic gonadotropin (Sigma) into the dorsal lymph sac of each frog. Approximately 12 h later, eggs were stripped into a dry Petri dish and fertilized by overlaying them with a suspension of approximately one-eighth of a minced

The publication costs of this article were defrayed in part by page charge payment. This article must therefore be hereby marked "*advertisement*" in accordance with 18 U.S.C. §1734 solely to indicate this fact.

0027-8424/97/941224-6$2.00/0
PNAS is available online at **http://www.pnas.org**.

Abbreviations: 1/3 MR, one-third strength modified amphibian Ringer's solution; $DiOC_6(3)$, 3,3′-dihexyloxacarbocyanine iodide; APC, adenomatous polyposis coli; ^2H_2O, deuterium oxide.

§To whom reprint requests should be addressed. e-mail: larabell@lbl.gov.

testis in 1–2 ml of one-third strength modified amphibian Ringer's solution (1/3 MR) (100% MR = 100 mM NaCl, 2 mM KCl, 1 mM $MgCl_2$, 2 mM $CaCl_2$, 50 μg/ml gentamycin, and 5 mM Hepes adjusted to pH 7.2 with NaOH). Fertilization was allowed to proceed for 6–8 min before de-jellying eggs with 2.5% cysteine hydrochloride in 1/3 MR adjusted to pH 8.0 with NaOH. Eggs were then rinsed 3–5 times with fresh 1/3 MR.

Treatment of Specimens with Vital Dyes and ^2H_2O. All treatments were performed immediately after eggs were fertilized and de-jellied. Organelles were labeled by staining eggs for 5 min in 1/3 MR containing 1 μg/ml nile red (Polysciences) (18) and 2 μg/ml $DiOC_6(3)$ [3,3′-dihexyloxacarbocyanine iodide (19); a gift to J.C.G from M. Terasaki (University of Connecticutt Health Center, Farmington, CT)] and then were removed and rinsed 2–3 times in fresh 1/3 MR. For ^2H_2O treatments, eggs were placed in 1/3 MR containing 70% ^2H_2O (Sigma) for 4 min, then rinsed 2–3 times in fresh 1/3 MR.

Confocal Microscopy of Live Eggs. Viewing dishes were made by replacing the bottom of a plastic Petri dish with a #1 glass coverslip (Baxter Health Care, Mundelein, IL), pouring in a thin layer of low gelling temperature agarose (Sigma) in 1/3 MR, and using 1.6-mm diameter steel balls to produce specimen wells in the molten agarose. After the agarose had cooled, the steel balls were removed, and the dish was filled with a solution of 5% Ficoll (Sigma) in 1/3 MR before placing eggs in the wells (20). Images were obtained with an inverted Leitz DM-IRB microscope with a × 40 objective (Leica, Heidelberg); others were obtained with an MRC-1000 laser scanning confocal microscope (Bio-Rad) equipped with an inverted Nikon (Tokyo) Diaphot 200 microscope and a × 60 PlanApo oil immersion objective lens (1.4 numerical aperture). The cell surface was identified by $DiOC_6(3)$ labeling, and optical sections were then collected by stepping inward at 0.2- to 0.5-μm intervals. Images were analyzed using Molecular Dynamics ImageSpace 3.10 software on a Silicon Graphics (Mountain View, CA) Indigo workstation. Fig. 1 *C* and *D* were prepared using Adobe Photoshop (San Jose, CA), overlaying images *A* and *B* after highlighting either yolk platelets (*C*) or $DiOC_6(3)$-labeled organelles (*D*).

Injection of Fluorescent Beads. Yellow–green FluoSpheres, 0.2 μm in diameter and coated with a hydrophilic polymer containing multiple carboxylic acids (Molecular Probes), were suspended 1:1 in distilled water, centrifuged, and resuspended to remove sodium azide. Immediately after the eggs were fertilized, 2–4 nl of washed FluoSpheres were injected by inserting a glass microneedle at the ventral equator and positioning the tip at the vegetal pole as close as possible to the inner surface of the plasma membrane. Some embryos were monitored live during cortical rotation using confocal microscopy, and others were fixed at the end of cortical rotation at the onset of first cleavage. After fixation (see below), eggs were cut in half with a microscalpel (Miltex Instruments, Lake Success, NY) along the animal–vegetal axis perpendicular to the cleavage furrow to obtain dorsal and ventral halves. Each half was sandwiched between two coverslips and flattened (final thickness ≈100 μm) so that the entire egg surface, from the vegetal pole to the equator, was in contact with the coverslip and at the same plane for viewing with the confocal microscope. Optical sections were then collected (using a ×10 lens) starting at the cell surface and moving into the cytoplasm so that the transport zone containing the microtubules and the streak of fluorescent beads could be visualized. The final image represents a projection of these sections (an image obtained by stacking successive optical sections on top of each other) and shows the entire streak of beads.

Whole Mount Immunocytochemistry. Eggs were fixed overnight in 4% paraformaldehyde, 0.1% glutaraldehyde, 100 mM KCl, 3 mM $MgCl_2$, 10 mM Hepes, 150 mM sucrose, and 0.1% Triton X-100 (pH 7.6). Nonspecific binding was blocked with 0.1% Triton X-100 in Super Block (Pierce). Specimens were then incubated overnight with a mouse monoclonal anti-β-tubulin antibody (Calbiochem) and/or an antibody raised in rabbit against a bacterial fusion protein derived from the amino-terminal region of *Xenopus* β-catenin (21). Secondary antibodies were fluorescein isothiocyanante-conjugated anti-mouse and tetramethylrhodamine B isothiocyanate-conjugated anti-rabbit (Sigma). Eggs were viewed with a Bio-Rad 1024 confocal laser scanning microscope using fluorescein filters to visualize microtubules and rhodamine filters to visualize β-catenin. Fluorophores were excited (and images obtained) sequentially to avoid bleed through of fluorescein into rhodamine.

RESULTS

Organelle Movements. When the cortex of an intact egg is immobilized, yolk platelets (labeled with nile red, rhodamine channel) in the cytoplasmic core move away from the prospective dorsal side at a uniform velocity of ≈10 μm/min (20, 22). We examined equivalent eggs treated with $DiOC_6(3)$, a lipophilic dye that labels membrane-bound organelles such as mitochondria and endoplasmic reticulum (19) and germ plasm in *Xenopus* eggs (23), and found that the $DiOC_6(3)$-labeled organelles (1–5 μm in diameter) deeper than 8 μm from the egg surface moved smoothly with the cytoplasmic core. Those organelles in the most peripheral region (≤4 μm deep) remained stationary, and, if the egg had not been immobilized, these organelles would have moved toward the prospective dorsal side at the same velocity as the cortex (≈10 μm/min).

However, in the zone 4–8 μm from the egg surface, where previous studies have shown that the microtubules of the parallel array are located (20), the most remarkable and previously unrecognized organelle movements were detected. In this zone, ≈10% of the $DiOC_6(3)$-labeled organelles moved rapidly toward the dorsal side (in the opposite direction of the yolk platelets and 90% of the $DiOC_6(3)$-labeled organelles) at velocities of 25–40 μm/min relative to the immobilized cortex (or 35–50 μm/min relative to the microtubule array that moves with the core). In a nonimmobilized egg, therefore, the organelles would be moving toward the prospective dorsal side more than three times as fast as the cortex moves (Fig. 1). These rapidly moving organelles undergo repeated, unidirectional saltations characteristic of microtubule, motor-driven transport rather than Brownian motion. Such movements occur only after the parallel array has formed and only in the zone occupied by the array (4–8 μm inside the vegetal surface). We were able to follow individual saltations over distances up to 40 μm, at which point the particles were no longer in the field of view. Thus, a transport zone exists at the interface of the cortex and inner cytoplasmic core where microtubules abound.

In $DiOC_6(3)$-stained eggs treated immediately after fertilization with UV irradiation or 50 μg/ml nocodazole (both of which disrupt microtubules and block cortical rotation), we saw no organelle movements other than random Brownian motion. When we treated fertilized eggs with ^2H_2O, we observed $DiOC_6(3)$-labeled organelles moving rapidly in all directions instead of uniformly opposite the direction of yolk platelet movement (Fig. 2). The organelles moved at least as rapidly, and as far, as in normal eggs.

Fluorescent Bead Transport. Immobilizing live eggs makes it impossible to image movements beyond the immediate vegetal pole region (≈200 μm in diameter), so we used another approach to determine whether these rapid, recurrent movements were capable of transporting organelles all the way to the dorsal equator. Previous investigators have shown that small carboxylated beads injected into axons and other cells move toward the plus ends of microtubules (24, 25), presumably transported by plus end-directed motor molecules. It also

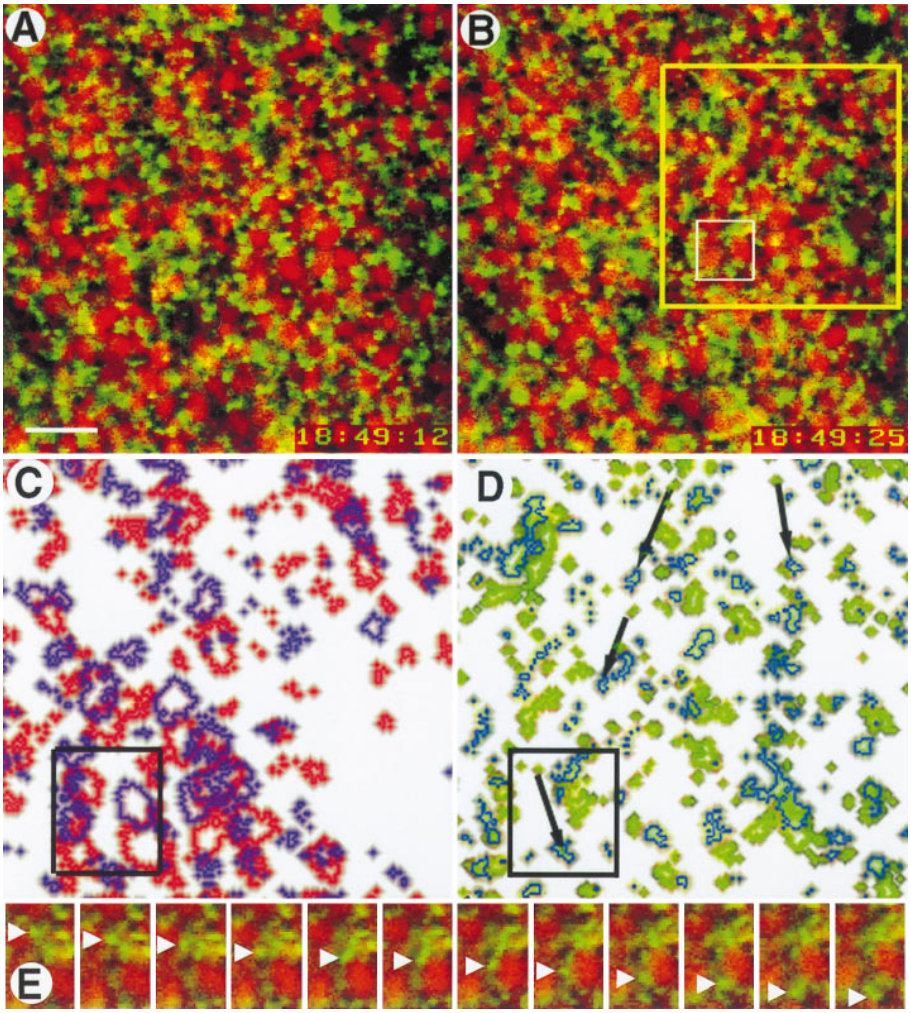

FIG. 1. Rapid movement of $DiOC_6(3)$-labeled organelles in the vegetal pole region of an egg during cortical rotation. Optical sections were collected at a frequency of one per second 4–8 μm inside the vegetal surface and then compiled into a time-lapse video. (*A* and *B*) The two images shown here were collected 13 sec apart. The red ovals are nile red-stained yolk platelets; between the time of the first image and the second, they have moved toward the upper left at a velocity of ≈10 μm/min. The smaller green circles are $DiOC_6(3)$-labeled organelles; between the first and second images, most of them have moved toward the upper left (with the yolk platelets), but ≈10% have moved in the opposite direction at ≈30 μm/min. Organelles were continuously tracked through the intervening images. The yellow box (*B*) outlines the region shown in *C* and *D*; the white box in *B* outlines the region shown in *E*. (*C*) Compiled image of a portion of *A* and *B* (yellow box, *B*), at slightly higher magnification, showing change in position of yolk platelets from *A* (red outlines) to *B* (purple outlines). (*D*) Compiled image of a comparable portion of *A* and *B* (yellow box, *B*) at slightly higher magnification showing change in position of $DiOC_6(3)$-labeled organelles from *A* (green outlines) to *B* (blue outlines). The black arrows indicate the routes taken by some of the 10% of small organelles that moved rapidly in the opposite direction of yolk platelet movement. The black boxes in *C* and *D* correlate with the white box shown in *B*. (*E*) Close-ups taken 1 sec apart in the interval between *A* and *B* showing a $DiOC_6(3)$-labeled organelle (green, white arrowheads) moving from top to bottom and a nile red-labeled yolk platelet (red) moving from bottom to top. By the 12th image, the small organelle has moved more than twice as far as the yolk platelet (Bar = 10 μm.)

is known that the plus ends of most microtubules in the parallel array in frog eggs point toward the future dorsal side (26). We injected carboxylated fluorescent beads into the vegetal pole region of immobilized eggs immediately after fertilization and used confocal microscopy to monitor their initial movement along microtubules near the vegetal pole.

In live eggs, most of the beads moved in the same direction and with the same velocity as the cytoplasmic core and microtubule array. Approximately 10% of the beads, however, traveled toward the future dorsal side of the egg at the velocity of the rapidly moving $DiOC_6(3)$-labeled organelles described above. After rotation, the eggs were fixed, bisected, and examined with the confocal microscope to measure the greatest extent of displacement of the beads. Several eggs (five of seven) showed a streak of fluorescent beads extending from the vegetal pole toward the equator, on the side of the egg opposite the sperm entry point (i.e., the probable future dorsal side). These streaks were between 526 and 692 μm long, with an average of 608 μm (corresponding to an angular distance of ≈60°). Optical sections showed that the beads were 4–8 μm inside the cell surface in the same region as the parallel array of microtubules and the organelle transport zone and that the width of the streaks was approximately equal to the diameter of the bolus of injected beads (Fig. 3). This suggests that components located at the vegetal pole before rotation can be transported along the parallel array of microtubules at least twice as far as they would be by the rotating cortex alone.

Localization of β-Catenin. Although the identity of the dorsal determinant(s) is unknown, one likely candidate is β-catenin, a component of the Wnt signal transduction pathway (*i*) that is present as both a maternal mRNA and protein, (*ii*) that is known to have dorsalizing activity in *Xenopus*, and (*iii*) whose elimination leads to ventralization (8, 12, 13). Using immunocytochemistry, we found that β-catenin is present on the future dorsal, but not ventral, side of the egg by the end of cortical rotation (Fig. 4). β-catenin forms a semicircular patch that is ≈60° wide and

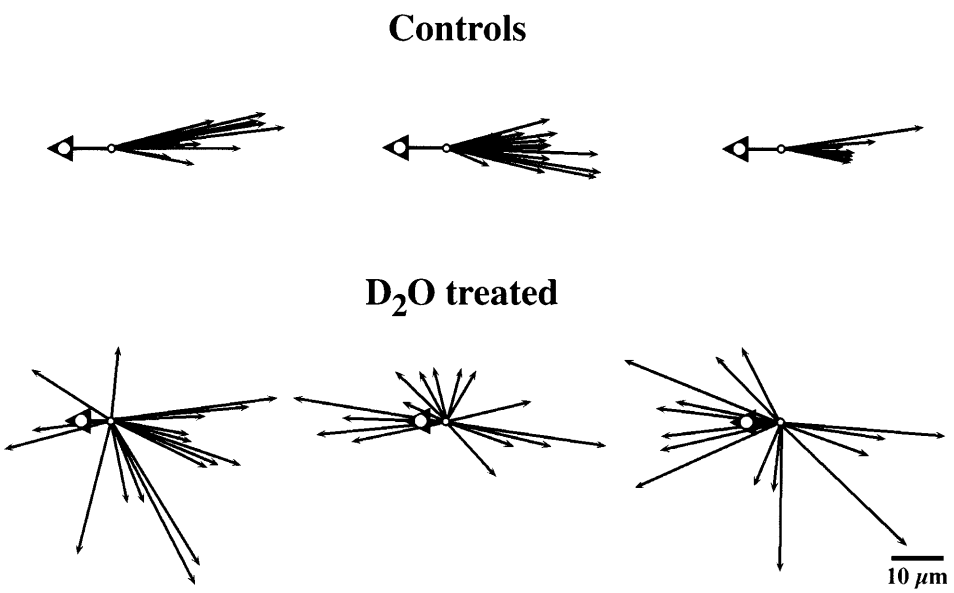

FIG. 2. Direction of organelle displacements 4–8 μm inside the vegetal surface of immobilized eggs undergoing cortical rotation. Arrowheads indicate the direction of yolk platelet movements that, in control eggs, averaged 11.3 μm. In ^2H_2O-treated eggs, yolk platelet displacement ranged between 0.3 and 12.2 μm, with an average displacement of 5.4 μm (n = 12). Arrows show the directions of rapidly moving $DiOC_6(3)$-labeled organelles. All vectors are brought to a common origin, and the length of the arrows is proportional to the distance traveled by the organelle before it stopped or left the field of view. Only displacements ≥ 3 μm were scored. In control eggs, the rapidly moving organelles are uniformly transported in the opposite direction from the yolk platelets; in ^2H_2O-treated eggs, their direction of movement is randomized away from the vegetal pole. Randomized movement also was seen in an additional six ^2H_2O-treated eggs (not shown here). (D_2O = ^2H_2O.)

located 60–90° from the vegetal pole. The patch is subsequently bisected by the cleavage furrow in most eggs. β-catenin localization is restricted to the 4- to 8-μm thick subcortical "transport zone" occupied by the microtubules (20) and appears to colocalize with the microtubules or occupy a volume adjacent to the microtubules. Secondary antibodies alone did not label eggs; antibodies to α-spectrin, protein 4.1, and ankyrin (which label the cell surface) did not label the microtubule array nor did they preferentially label components of the transport zone on the dorsal side (data not shown).

DISCUSSION

Previously, it was thought that dorsalization of one side of the frog egg was caused by factors attached to the cortex and transported by it as it moved along aligned microtubules (toward the plus ends), driven by attached motor molecules. Because the cortex moves 30°, the extent of transport would be no greater than this movement. Cytoplasmic transfer experiments suggest, however, that dorsalizing components are transported from the vegetal pole to the equator, a displacement approximately three times greater than that of cortical rotation (4, 5).

We show here that the microtubules can, independent of the cortex, function in the rapid and extensive directional transport of small organelles (1–5 μm diameter) to an equatorial sector 60–90° from the vegetal pole that later develops into dorsoanterior structures. Small, endogenous, $DiOC_6(3)$-labeled organelles (which include endoplasmic reticulum and mitochon-

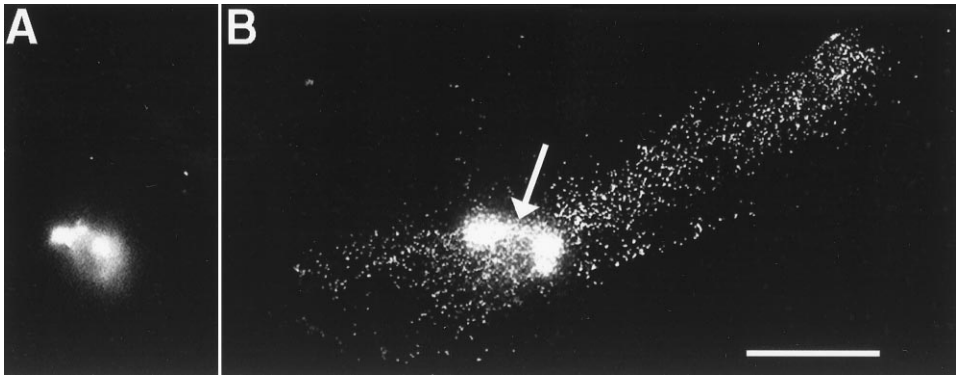

FIG. 3. Movement of fluorescent beads from the vegetal pole to the equatorial region during cortical rotation. (*A*) A bolus of beads at the vegetal pole before the onset of cortical rotation. (*B*) A streak of beads in an egg fixed at the end of cortical rotation, when the first cleavage furrow has begun to form. A linear array of beads is seen extending ≈600 μm from the center of the bolus of beads at the vegetal pole (arrow) toward the equator on the side of the egg opposite the sperm entry point, where the future dorsal side usually forms. Fixed eggs were cut in half along the animal–vegetal axis perpendicular to the cleavage furrow, and each half was compressed between two coverslips (to a final thickness of ≈100 μm) to facilitate visualization of the future dorsal and ventral halves. Optical sections were collected at 0.2-μm intervals, starting at the cell surface and moving into the cytoplasm, to visualize the entire transport zone located 4–8 μm from the cell surface. The final image represents a projection of these sections and shows the entire streak of beads. In some eggs (not shown), beads leaked from the injection needle into the deep cytoplasm between the injection site and the vegetal pole. These streaks were easily distinguished from streaks caused by cortical rotation because they were in the half of the egg containing the sperm entry site, were several hundred microns deeper in the cytoplasm, and were more visible from the bisected cytoplasmic side of the egg than from the plasma membrane. (Bar = 200 μm.)

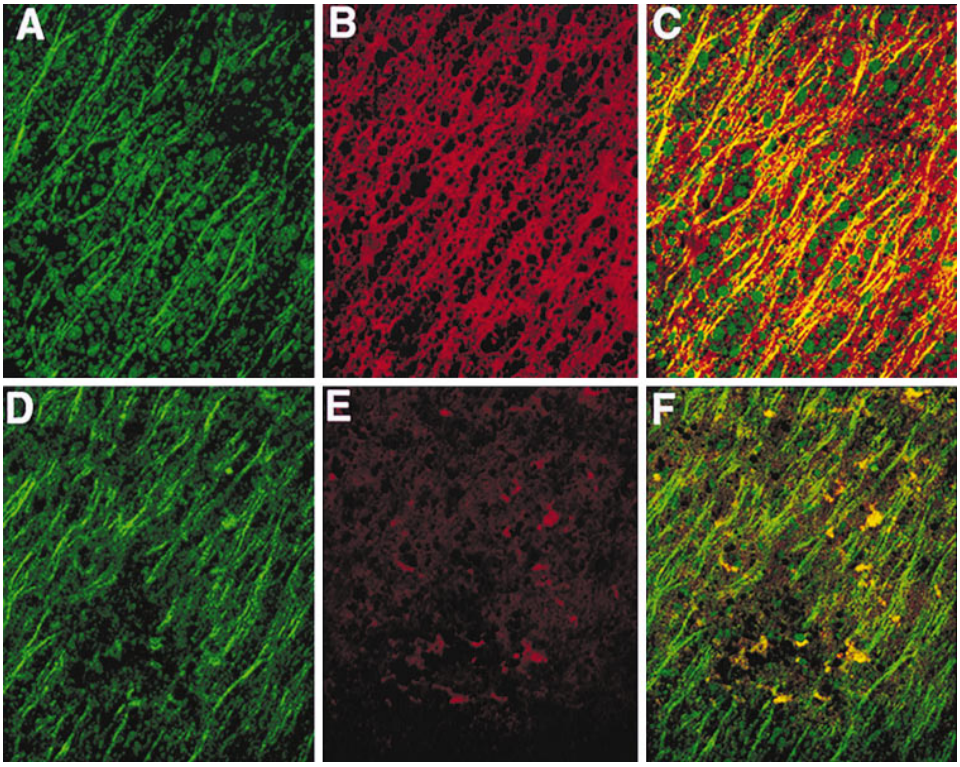

FIG. 4. Colocalization of β-catenin with subcortical microtubules on the future dorsal side of *Xenopus* eggs at the end of cortical rotation (0.8 of the first cell cycle). Images show labeling with antibodies to β-tubulin and β-catenin ($n = 9$). (*A*) Microtubules (green) of the parallel array on the future dorsal side 60–90° from the vegetal pole; (*B*) linear array of β-catenin (red) in the same region 4–8 μm from the cell surface; (*C*) colocalization of microtubules and β-catenin (yellow) in this region; (*D*) microtubules (green) on the future ventral side 60–90° from the vegetal pole; (*E*) this same (ventral) region shows only small isolated patches of β-catenin; and (*F*) linear pattern is green rather than yellow (in contrast to *C*), indicating no colocalization of β-catenin with microtubules on the ventral side. (Bar = 50 μm).

dria; ref. 19) within the microtubule array in the transport zone are unattached to the cortex and are rapidly transported toward the future dorsal side at a velocity approximately three times greater than that of the cortex. Although our methods did not enable us to follow these organelles beyond the vegetal pole region, we could observe that injected carboxylated beads were transported ≈60° from the vegetal pole toward the dorsal equator, a distance twice that of cortical rotation. These results suggest that at least some dorsal determinants are not transported by the moving cortex but are transported to the equator by microtubule motor molecules traveling toward the plus ends of microtubules of the parallel array.

From these data, we propose a new model for the way in which cortical rotation initiates specification of the dorsal–ventral axis. In this model, the 30° cortical/cytoplasmic displacement aids in the alignment of microtubules into a parallel array that then serves as a directional transport system. The cortex travels along the transport system at 10 μm/min whereas dorsalizing components travel along these microtubules at 35–50 μm/min, in the same direction as the cortex. The plus end-directed movements and the velocities of the organelles are characteristic of transport by kinesin-like motor proteins. Using this rapid transport system, dorsalizing components located at the vegetal pole before rotation can travel to the equatorial region (a 90° displacement), which, as a result, develops into a Nieuwkoop center that later induces an organizer that patterns and contributes to dorsoanterior structures (Fig. 5). Some transported components would serve in forming the Nieuwkoop center and others in the enhanced responsiveness of dorsal animal blastomeres to inductive signals from the center. Dorsally directed movements of organelles also have been observed in medaka eggs (27).

^2H_2O tends to randomize the orientation of microtubules in the transport zone and reduces the extent of cortical rotation in frog eggs, yet paradoxically it broadens the zone of dorsalization (2). We found that ^2H_2O randomizes the direction of movement of small endogenous organelles away from the vegetal pole, the kinds of organelles that would normally be rapidly transported in a single direction. Hence, organelles initially located at the vegetal pole could be transported to all sectors of the equator. If some of those organelles carry dorsal determinants, this randomization could explain how ^2H_2O broadens the zone of dorsalization even though the cortex moves less. Vegetal microtubules are still present, so the nonrotating, ^2H_2O-treated egg is basically different from the nonrotating, UV-treated egg, which lacks microtubules.

Although the identity of the dorsal determinant(s) that might be traveling on the microtubules is not known, components of the Wnt signaling pathway are potential candidates. We focused on β-catenin because it is both necessary (14) and sufficient (13, 15) for dorsoanterior axis specification. We found that, at the end of rotation, cytoplasmic β-catenin is enriched on the future dorsal side in a semicircular patch subequatorially in the vegetal hemisphere 60–90° from the vegetal pole. The β-catenin is arranged in a linear pattern, in the same direction as the microtubules, and is restricted to the microtubule-rich transport zone 4–8 μm from the cell surface. It appears to colocalize extensively with the microtubules as if it associates with them. Whereas it is possible that β-catenin merely occupies the yolk-free space in the 4–8 μm transport zone, it is difficult to imagine that any protein or organelle could remain in this turbulent zone if it was not in some way associated, directly or indirectly, with the microtubules of that zone.

The apparent colocalization of β-catenin and microtubules at the future dorsal side at the end of rotation raises the possibility that this protein is transported along the microtubules during cortical rotation and then participates in axis

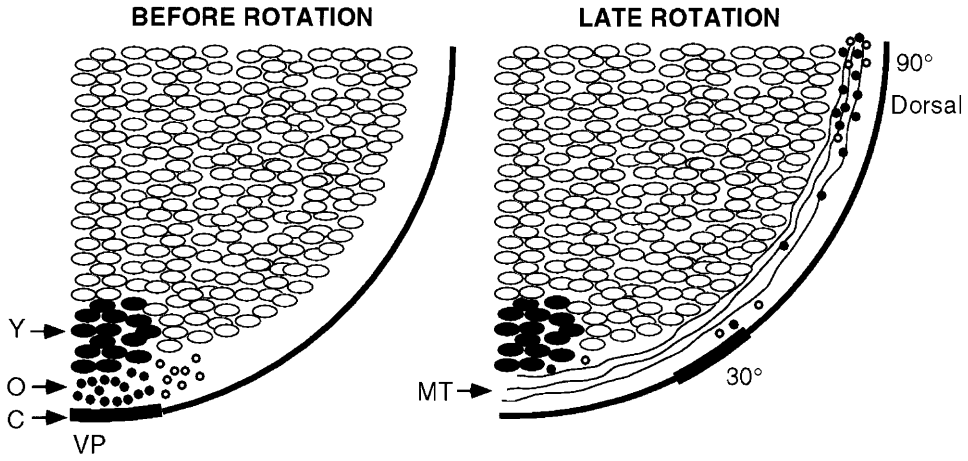

FIG. 5. Model of microtubule-mediated rapid transport of dorsalizing components in a free-floating (nonimmobilized) egg. (*Left*) The highlighted region at the vegetal pole represents a spot [labeled with nile red and $DiOC_6(3)$] before cortical rotation [Y, yolk platelets; O, small organelles (●, labeled; ○, unlabeled); C, cortex; VP, vegetal pole]. (*Right*) The location of various components near the end of rotation are shown on the right (MT, microtubules). The core of yolk platelets remains oriented downward, the cortex moves ≈30° along the microtubules, and some organelles in the microtubule transport zone (4–8 μm from the cell surface) move ≈90° along microtubules to the equatorial region on the future dorsal side of the embryo.

specification. However, β-catenin is rapidly degraded as a result of phosphorylation by Xgsk-3 (21), and its dorsal accumulation may represent local stabilization rather than transport. It is possible that Xgsk-3, or a component affecting its activity, is translocated on microtubules to generate dorsal–ventral differences in the activity of Xgsk-3, thereby effecting β-catenin stability and the observed dorsal–ventral differences in β-catenin distribution. Although β-catenin does not have a known microtubule-binding domain, it does bind to the adenomatous polyposis coli (APC) protein, which does associate with microtubules *in vitro* and *in vivo* (28–30). The role of APC in Wnt signaling in *Xenopus* has not yet been demonstrated, but it is implicated by the fact that Wnt1 signals in cultured cells increase the steady-state levels of APC protein as well as stabilize APC–catenin complexes (31). APC may be involved in the colocalization of locally stabilized β-catenin to the microtubules of the parallel array. Whether the β-catenin associated with microtubules in the dorsal vegetal cortex is sufficient to directly initiate axis formation is unclear, but it may serve to initiate the later accumulation of β-catenin in the dorsal blastomeres, which in turn effects axis formation (17).

We thank Frank Lie of Leica for valuable technical assistance. This work was supported by the Office of Health and Environmental Research, U.S. Department of Energy (C.A.L.), and by National Institutes of Health Grant RO1 GM19363 (J.C.G.). R.T.M. was supported as an investigator of the Howard Hughes Medical Institute.

1. Elinson, R. P. & Rowning, B. (1988) *Dev. Biol.* **128,** 185–197.
2. Gerhart, J. C., Danilchik, M., Doniach, T., Roberts, S., Rowning, B. & Stewart, R. (1989) *Development (Cambridge, U.K.)* **107,** Suppl., 37–51.
3. Elinson, R. P. & Holowacz, T. (1995) *Curr. Top. Dev. Biol.* **30,** 253–285.
4. Fujisue, M., Kobayakawa, Y. & Yamana, K. (1993) *Development (Cambridge, U.K.)* **118,** 163–170.
5. Holowacz, T. & Elinson, R. P. (1993) *Development (Cambridge, U.K.)* **119,** 277–285.
6. Sakai, M. (1996) *Development (Cambridge, U.K.)* **122,** 2207–2214.
7. Scharf, S. R., Rowning, B., Wu, M. & Gerhart, J. C. (1989) *Dev. Biol.* **134,** 175–188.
8. DeMarais, A. A. & Moon, R. T. (1992) *Dev. Biol.* **153,** 337–346.
9. Du, S., Purcell, S., Christian, J., McGrew, L. & Moon, R. (1995) *Mol. Cell. Biol.* **15,** 2625–2634.
10. Moon, R. T., Christian, J. L., Campbell, R. M., McGrew, L. L., DeMarais, A. A., Torres, M., Lai, C. J., Olson, D. J. & Kelly, G. M. (1993) *Development (Cambridge, U.K.)*, Suppl., 85–94.
11. Cui, Y., Brown, J. D., Moon, R. T. & Christian, J. L. (1995) *Development (Cambridge, U.K.)* **121,** 2177–2186.
12. Fagotto, F., Funayama, N., Gluck, U. & Gumbiner, B. (1996) *J. Cell Biol.* **132,** 1105–1114.
13. Guger, K. A. & Gumbiner, B. M. (1995) *Dev. Biol.* **172,** 115–125.
14. Heasman, J., Crawford, A., Goldstone, K., Garner-Hamrick, P., Gumbiner, B., McCrea, P., Kintner, C., Noro, C. Y. & Wylie, C. (1994) *Cell* **79,** 791–803.
15. Kelly, G. M., Greenstein, P. E., Erezyilmaz, D. F. & Moon, R. T. (1995) *Mech. Dev.* **53,** 261–273.
16. Schneider, S., Steinbeisser, H., Warga, R. M. & Hausen, P. (1996) *Mech. Dev.* **57,** 191–198.
17. Larabell, C. A., Torres, M., Rowning, B. A., Yost, C. A., Miller, J. R., Wu, M., Kimelman, D. & Moon, R. T. (1997) *J. Cell Biol.*, in press.
18. Greenspan, P., Mayer, E. P. & Fowler, S. D. (1985) *J. Cell Biol.* **100,** 965–973.
19. Terasaki, M., Song, J., Wong, J. R., Weiss, M. J. & Chen, L. B. (1984) *Cell* **38,** 101–108.
20. Larabell, C. A., Rowning, B. A., Wells, J., Wu, M. & Gerhart, J. C. (1996) *Development (Cambridge, U.K.)* **122,** 1281–1289.
21. Yost, C., Torres, M., Miller, J. R., Huang, E., Kimelman, D. & Moon, R. T. (1996) *Genes Dev.* **15,** 1443–1454.
22. Vincent, J.-P., Oster, G. F. & Gerhart, J. C. (1986) *Dev. Biol.* **113,** 484–500.
23. Savage, R. M. & Danilchik, M. V. (1993) *Dev. Biol.* **157,** 371–382.
24. Terasaki, M., Schmidek, A., Galbraith, J. A., Gallant, P. E. & Reese, T. S. (1995) *Proc. Natl. Acad. Sci. USA* **92,** 11500–11503.
25. Adams R. J. & Bray, D. (1983) *Nature (London)* **303,** 718–720.
26. Houliston, E. & Elinson, R. P. (1991) *J. Cell Biol.* **114,** 1017–1028.
27. Trimble, L. M. & Fluck, R. A. (1995) *Fish. Biol. J. (Medaka)* **7,** 37–41.
28. Su, L. K., Vogelstein, B. & Kinzler, K. W. (1993) *Science* **262,** 1734–1737.
29. Rubinfeld, B., Souza, B., Albert, I., Müller, O., Chamberlain, S. H., Masiarz, F. R., Munemitsu, S. & Polakis, P. (1993) *Science* **262,** 1731–1734.
30. Munemitsu, S., Albert, I., Souza, B., Rubinfeld, B. & Polakis, P. (1995) *Proc. Natl. Acad. Sci. USA* **92,** 3046–3050.
31. Papkoff, J., Rubinfeld, B., Schryver, B. & Polakis, P. (1996) *Mol. Cell. Biol.* **16,** 2128–2134.